CERN-TH-2002-023

arXiv:hep-th/0203006 v2 18 Mar 2002

Critical exponents from optimised renormalisation group flows

Daniel F. Litim

Theory Division, CERN, CH – 1211 Geneva 23.
(Daniel.Litim@cern.ch)

Abstract

Within the exact renormalisation group, the scaling solutions for O(N) symmetric scalar field theories are studied to leading order in the derivative expansion. The Gaussian fixed point is examined for $d > 2$ dimensions and arbitrary infrared regularisation. The Wilson-Fisher fixed point in $d = 3$ is studied using an optimised flow. We compute critical exponents and subleading corrections-to-scaling to high accuracy from the eigenvalues of the stability matrix at criticality for all N. We establish that the optimisation is responsible for the rapid convergence of the flow and polynomial truncations thereof. The scheme dependence of the leading critical exponent is analysed. For all $N \geq 0$, it is found that the leading exponent is bounded. The upper boundary is achieved for a Callan-Symanzik flow and corresponds, for all N, to the large-N limit. The lower boundary is achieved by the optimised flow and is closest to the physical value. We show the reliability of polynomial approximations, even to low orders, if they are accompanied by an appropriate choice for the regulator. Possible applications to other theories are outlined.

I. INTRODUCTION

Renormalisation group techniques are important tools to describe how classical physics is modified by quantum fluctuations. Integrating-out all quantum fluctuations provides the link between the classical theory and the full quantum effective theory. Universality implies that the details of the underlying classical theory – other than the global symmetries, long- or short-range interactions, and the dimensionality – are irrelevant for the characteristics of the quantum effective theory. For this reason, universal properties of phase transitions in numerous physical systems (entangled polymers, liquid-vapour transition, superfluid transition in ^{4}He, ferromagnetic transitions, QCD phase transition with two massless quark flavours) can be addressed based on simple scalar field theories [1].

A useful method is given by the Exact Renormalisation Group (ERG) [2–6], which is based on the Wilsonian idea of integrating-out infinitesimal momentum shells. The corresponding flow, which has a simple one-loop structure, is very flexible concerning approximations, and its domain of applicability is not tied to weak coupling. Recently, it has been shown that ERG flows can be optimised, thereby providing improved results already to low orders within a given approximation [7–10]. In the present paper, we apply this idea to the universality class of $O(N)$ symmetric scalar theories in three dimensions and compute critical exponents and subleading corrections to scaling. We expect that insights gained from this investigation will also prove useful for applications to gauge theories [11] or gravity [12], which are more difficult to handle.

Universal critical exponents have been computed previously using either polynomial truncations of exact renormalisation group flows, or the derivative expansion to leading and subleading order [10,13–24], and in [24,25] based on the proper-time renormalisation group [26]. All results are affected by the underlying approximations which induce a spurious dependence on the regularisation [10,17,22,27–29]. This is somewhat similar to the scheme dependence within perturbative QCD, or within truncated solutions of Schwinger-Dyson equations. While this scheme dependence should vanish at sufficiently high order in the expansion, practical applications are always bound to a finite order, and hence to a non-vanishing scheme dependence. In some cases, it has even been observed that higher order results happen to be worse than lower order ones [21]. In consequence, one should gain some understanding of the spurious scheme dependence. Without this, it is difficult to decide which of the different scheme-dependent results within a fixed truncation could be considered as trustworthy.

A partial understanding of the interplay of approximations and scheme dependence has been achieved previously. For scalar QED [30], the scheme dependence in the region of first order phase transition has been studied in [28,29]. For $3d$ scalar theories, the interplay between the smoothness of the regulator and the resulting critical exponents has been addressed in [22] using a minimum sensitivity condition. For Einstein quantum gravity, where

a new UV fixed point has been found recently to low orders in a polynomial truncation, the corresponding analysis has been given in [31]. The weak scheme dependence found in these cases suggests that higher order corrections remain small, thereby strengthening the results existing so far. The evidence created this way is partly circumstantial, because the range over which a physical observable varies with the scheme depends on the class of regulators.

Here, we address the problem from a different perspective. The main ingredient in our analysis is the concept of optimisation [7–10]. For a given physical problem, it should be possible to identify specific regulators which lead to a better convergence behaviour of the flow. This strategy is based only on the ERG flow itself and has lead to a simple optimisation criterion for flows [7]. Optimised flows have a number of interesting properties [8]. They lead to a fast decoupling of heavy modes, they disentangle quantum and thermal fluctuations along the flow, and they lead to a smooth approach towards a convex effective potential for theories in a phase with spontaneous symmetry breaking. The optimisation is closely linked to a minimum sensitivity condition [9] in a sense which will be made transparent below. Furthermore, optimised flows have been shown to improve the convergence of the derivative expansion [10]. Thus, optimised flows are promising candidates for high precision computations within this formalism. Here, we do so within a local potential approximation.

The second new ingredient of our analysis consists in a study of the largest possible range of flows, and the corresponding critical exponents. We find that the range is larger than previously assumed. Furthermore, the results from optimised flows are located at the (lower) boundary and happen to be closest to the physical values.

For the numerical analysis, and apart from the local potential approximation, we employ a polynomial approximation. This additional approximation is reliable if it converges reasonably fast towards the full solution. However, it has been criticised previously in the literature. For a sharp cut-off, it has lead to spurious solutions [14], and its convergence was found to be poor [32], which has lead to strong doubts concerning its reliability (see also [33]). In contrast to these findings, we show that the poor convergence is an artifact of the sharp cut-off regulator, rather than an artifact of the polynomial approximation. Using an optimised flow, we find that the polynomial approximation is stable and that it converges rapidly for all technical purposes.

The format of the paper is as follows. We review the basic ingredients of the formalism and introduce the optimisation ideas (Sect. II). Then, we introduce our numerical method and study the non-trivial scaling solution in $3d$ (Sect. III). We compute the eigenvalues at criticality to high accuracy from an optimised flow. The convergence and stability of the flow, and of the polynomial truncation, are established (Sect. IV). We study the scheme dependence of the critical index ν (Sect. V). Finally, we discuss the main results of the paper with particular emphasis on the predictive power, on the convergence properties of flows, and on implications for other theories (Sect. VI). Three appendices contain the study

of the Gaussian fixed point for arbitrary regularisation and $d > 2$ (App. A), and technical details for specific classes of regulators, including a computation of the corresponding flows and critical exponents (Apps. B and C).

II. RG FLOW FOR $O(N)$ SYMMETRIC SCALAR THEORIES

Here, we briefly review some basic ingredients of the ERG formalism, and its approximation to leading order in the derivative expansion. We also discuss important aspects of the regularisation, and its optimisation, which is employed in the following sections.

A. Renormalisation group flows

Exact renormalisation group equations are based on the Wilsonian idea of integrating out momentum modes within a path integral representation of quantum field theory [2]. In its modern form, the ERG flow for an effective action Γ_k for bosonic fields ϕ is given by the simple one-loop expression [3–6]

$$\partial_t \Gamma_k[\phi] = \frac{1}{2}\mathrm{Tr}\left(\frac{\delta^2\Gamma_k}{\delta\phi\,\delta\phi} + R_k\right)^{-1} \partial_t R_k \tag{2.1}$$

Here, $t \equiv \ln k$ is the logarithmic scale parameter, and $R_k(q^2)$ is an infrared (IR) regulator at the momentum scale k. From now on, we suppress the index k on R. The flow trajectory of Eq. (2.1) in the space of action functional depends on the IR regulator function R. R obeys a few restrictions, which ensure that the flow equation is well-defined, thereby interpolating between an initial action in the UV and the full quantum effective action in the IR. We require that

$$\lim_{q^2/k^2\to 0} R(q^2) > 0\,, \tag{2.2}$$

$$\lim_{k^2/q^2\to 0} R(q^2) \to 0\,, \tag{2.3}$$

$$\lim_{k\to\Lambda} R(q^2) \to \infty\,. \tag{2.4}$$

Equation (2.2) ensures that the effective propagator at vanishing field remains finite in the infrared limit $q^2 \to 0$, and no infrared divergences are encountered in the presence of massless modes. Equation (2.3) guarantees that the regulator function is removed in the physical limit, where $\Gamma \equiv \lim_{k\to 0}\Gamma_k$. Equation (2.4) ensures that Γ_k approaches the microscopic action $S = \lim_{k\to\Lambda}\Gamma_k$ in the UV limit $k \to \Lambda$. We put $\Lambda = \infty$ in the sequel. For later use, we introduce a dimensionless regulator function $r(y)$ as

$$R(q^2) = q^2\, r(q^2/k^2)\,. \tag{2.5}$$

Now we turn to the flow equation for an $O(N)$ symmetric scalar field theory in d dimensions to leading order in the derivative expansion, the so-called local potential approximation [34]. This approximation amounts to the Ansatz

$$\Gamma_k = \int d^d x \left(U_k(\bar{\rho}) + \frac{1}{2}\partial_\mu \phi^a \partial_\mu \phi_a \right) \ . \tag{2.6}$$

for the functional Γ_k. The Ansatz neglects higher order corrections proportional to the anomalous dimension η of the fields. The latter are of the order of a few percent for the physically interesting universality classes $N = 0, \cdots, 4$. Hence, we expect that a derivative expansion is sensible, and that the result of a leading order computation is correct up to corrections of the order of η. Inserting this Ansatz into (2.1) and evaluating it for constant fields leads to the flow for U_k. We rewrite this flow equation in dimensionless variables $u(\rho) = U_k/k^d$ and $\rho = \frac{1}{2}\phi^a\phi_a k^{2-d}$. In addition, the angular integration of the momentum trace is performed to give [35]

$$\partial_t u + du - (d-2)\rho u' = 2v_d(N-1)\ell(u') + 2v_d \ell(2\rho u'') \tag{2.7}$$

with $v_d^{-1} = 2^{d+1}\pi^{d/2}\Gamma(\frac{d}{2})$. The function $\ell(\omega)$ are given by

$$\ell(\omega) = \tfrac{1}{2}\int_0^\infty dy y^{d/2} \frac{\partial_t r(y)}{y(1+r)+\omega} \tag{2.8}$$

with $y \equiv q^2/k^2$ and $\partial_t r(y) = -2yr'(y)$. The flow (2.7) is a second order non-linear partial differential equation. All non-trivial information regarding the renormalisation flow and the regularisation scheme (RS) are encoded in the function (2.8). The momentum integration is peaked and regularised: for large momenta due to the regulator term $\partial_t r(y)$, and for small momenta due to $r(y)$ in the numerator. All terms on the left-hand side of Eq. (2.7) do not depend explicitly on the RS. They simply display the intrinsic scaling of the variables which we have chosen for our parametrisation of the flow.

B. Optimisation

A good choice for the regulator is most important for a rapid convergence and the stability of an approximated flow towards the physical theory. Recently, is has been argued that such (optimised) choices of the IR regularisation are indeed available [7–9]. The main observation is that the flow trajectory of (2.1) depends on the regularisation. This observation is most important for approximated flows: typically, their endpoint also depends spuriously on the regularisation. The dependence is absent for the full integrated flow. Hence, in order to provide reliable physical predictions, it is important to seek for regularisations for which the main physical informations are already contained within a few leading order terms of an approximation. This issue is intimately linked to the stability of flows.

The main ingredient in (2.1) is the full inverse propagator. Due to the IR regularisation, the full inverse regularised propagator displays a gap as a function of momenta [8,9],

$$\min_{q^2\geq 0}\left(\left.\frac{\delta^2\Gamma_k[\phi]}{\delta\phi(q)\delta\phi(-q)}\right|_{\phi=\phi_0}+R_k(q^2)\right)=C\,k^2>0\,. \tag{2.9}$$

The functional derivative is evaluated at a properly chosen expansion point ϕ_0. The existence of the gap $C>0$ implies an IR regularisation, and is a prerequisite for the ERG formalism. Elsewise, (2.1) becomes singular at points where the full inverse effective propagator develops zero modes. It is expected that an approximated ERG flow in the space of all action functionals is most stable if the regularised full propagator is most regular along the flow. This reasoning corresponds to maximising the gap.

To leading order in the derivative expansion, and dropping irrelevant momentum-independent terms, the gap is given by

$$C=\min_{y\geq 0}y(1+r(y))\,. \tag{2.10}$$

Within the local potential approximation, the gap C in (2.10) depends on the regularisation, but not on the specific theory considered. A comparison of the gap of different regulators requires an appropriate normalisation of r. In order to make the flow (2.1) more stable, we require that the gap, as a function of the RS, is maximal in the momentum regime where the flow receives its main contributions. This is the optimisation criterion of [7–9]. It corresponds to an optimisation of the radius of convergence of amplitude expansions and the derivative expansion. It can also be shown that the optimisation is closely linked to a minimum sensitivity condition. Optimised regulators are those for which the maximum in (2.10) is attained. In Ref. [8], these considerations have lead to a very specific solution to the optimisation condition, given by

$$R_{\rm opt}(q^2)=(k^2-q^2)\,\theta(k^2-q^2)\,. \tag{2.11}$$

It has a number of interesting properties. For large momenta $q^2>k^2$, the propagation of modes is fully suppressed since $R\equiv 0$. For small momenta $q^2<k^2$, all modes propagate with an effective mass term given by the IR scale, $q^2+R(q^2)=k^2$. Based on the discussion in Refs. [7–9], we expect that Eq. (2.11) leads to an improved convergence and hence better physical predictions already to leading order in the derivative expansion. Rewriting (2.11) in the form of (2.5) leads to

$$r_{\rm opt}(y)=(\tfrac{1}{y}-1)\,\theta(1-y) \tag{2.12}$$

Below, we mainly employ this regulator, and variants thereof (cf. Appendices B and C). When expressed in terms of the optimised regulator (2.11), the flow equation (2.7) becomes

$$\partial_t u = -du + (d-2)\rho u' + \frac{4}{d} v_d \frac{N-1}{1+u'} + \frac{4}{d} v_d \frac{1}{1+u'+2\rho u''} \,. \tag{2.13}$$

Notice that the numerical factors $(4v_d)/d$ can be absorbed into the potential and the fields by an appropriate rescaling.

III. FIXED POINTS

The flow equation (2.13) is known to exhibit two scaling solutions in $2 < d < 4$, which correspond to the Gaussian and the Wilson-Fisher fixed point, respectively. The Gaussian fixed point is given by the trivial solution $u_\star = \text{const}$, and is discussed in the Appendix A for arbitrary regularisation and $2 < d < 4$. In this section, we study the non-trivial fixed point $u_\star \neq \text{const.}$ in $3d$ based on an optimised flow. We introduce the numerical method, and discuss the scaling form of the fixed point solution. Universal critical exponents are computed in the next section.

A. Numerics

Numerical methods for solving partial differential equations are well-known. Here, we employ a polynomial truncation of the scaling potential, retaining vertex functions ϕ^{2n} up to a maximum number n_{trunc}. Polynomial approximations are reliable if they depend only very weakly on higher order operators beyond some finite order of the truncation. (In the following section, we explicitly confirm that this is indeed the case.) Two different polynomial expansions of the potential are used: expansion I corresponds to

$$u(\rho) = \sum_{n=1}^{n_{\text{trunc}}} \frac{1}{n!} \lambda_n \rho^n \,. \tag{3.1}$$

In Eq. (3.1), λ_1 denotes the (dimensionless) mass term at the origin. We have normalised the potential as $u(\rho = 0) = 0$. All higher order coefficients λ_n denote the n-th order coupling at vanishing field. Expansion II, alternatively, approximates the potential about the potential minimum $\rho = \rho_0$ as

$$u(\rho) = \sum_{n=2}^{n_{\text{trunc}}} \frac{1}{n!} \lambda_n (\rho - \lambda_1)^n \,. \tag{3.2}$$

In Eq. (3.2), λ_1 denotes the location of the potential minimum defined by $u'(\rho = \lambda_1) = 0$. We have normalised the potential as $u(\lambda_1) = 0$. All higher order coefficients λ_n denote the n-th order coupling at the potential minimum. Both expansions (3.1) and (3.2) are symmetric under $\phi \to -\phi$, and approximate the potential as an even polynomial in ϕ. The number of independent operators contained in Eq. (3.1) or Eq. (3.2) is n_{trunc}. The

expansions transform the partial differential equation (2.7) into $n_{\rm trunc}$ coupled ordinary differential equations $\partial_t \lambda_i \equiv \beta_i(\{\lambda_n\})$ for the set of couplings

$$\{\lambda_n, 1 \leq n \leq n_{\rm trunc}\}\,. \tag{3.3}$$

For the numerical study, we use mostly expansion II, which is known to have superior convergence properties in comparison to expansion I [33,7].

B. Wilson-Fisher fixed point

The Wilson-Fisher fixed point corresponds to the non-trivial scaling solution of (2.13). Here, we restrict ourselves to the case $d = 3$, and to the optimised regulator as introduced above. The scaling potential obeys the differential equation

$$0 = -3u_\star + \rho u_\star' + \frac{1}{6\pi^2}\frac{N-1}{1+u_\star'} + \frac{1}{6\pi^2}\frac{1}{1+u_\star'+2\rho u_\star''} + \text{const.} \tag{3.4}$$

and $u_\star(\rho) \neq$ const. The constant in Eq. (3.4) can be fixed freely, and we chose it such that the scaling potential vanishes at its minimum, $u_\star = 0$ at the point ρ_0 with $u_\star' = 0$. An analytical solution of Eq. (3.4) has been given in Ref. [18] for the limit $N = \infty$. For $N \neq \infty$, and in the vicinity of $\rho = 0$, the scaling solution can be obtained analytically as a Taylor expansion in the field. For $d = 3$ and $N = 1$, and inserting the expansion (3.1) into (3.4) with const. $= 0$, we find

$$\lambda_0 = \tfrac{1}{18}\pi^{-2}(1+\lambda_1)^{-1} \tag{3.5a}$$
$$\lambda_2 = -4\pi^2\,\lambda_1\,(1+\lambda_1)^2 \tag{3.5b}$$
$$\lambda_3 = \tfrac{72}{15}\pi^4\,\lambda_1\,(1+\lambda_1)^3\,(1+13\,\lambda_1) \tag{3.5c}$$
$$\lambda_4 = -\tfrac{1728}{7}\pi^6\,\lambda_1^2\,(1+\lambda_1)^4\,(1+7\,\lambda_1) \tag{3.5d}$$
$$\lambda_5 = \tfrac{768}{7}\pi^8\,\lambda_1^2\,(1+\lambda_1)^5\,(2+121\,\lambda_1+623\,\lambda_1^2) \tag{3.5e}$$
$$\vdots$$

for small fields. Similar explicit solutions are found for $d \neq 3$ or $N \neq 1$. Notice that all couplings are expressed as functions of the dimensionless mass term at vanishing field, λ_1. The domain of validity of this expansion is restricted to $0 \leq \rho \leq \rho_c < \infty$. From the explicit solution for large fields, (3.6) below, it is clear that the polynomial approximation cannot be extended to arbitrary large fields. The value ρ_c defines the radius of convergence for the polynomial approximation. It is linked to the gap parameter C introduced earlier [7]. Not all values for λ_1 lead to a scaling solution which remains finite and analytical for all $\rho < \rho_c$. It is at this point where the quantisation of λ_1 becomes manifest: only two values for λ_1 correspond to well-defined solutions of the fixed point equation, given by the Gaussian fixed point $\lambda_1 = 0$ and the Wilson-Fisher fixed point $\lambda_1 = \lambda_{1\star} < 0$. The value for $\lambda_{1\star}$ is

determined by fine tuning λ_1 such that the solution (3.5) extends to $\rho = \rho_c$. The result is $\lambda_{1\star} = -0.1860642\cdots$ for $N = 1$. In the other limit, for large fields $\rho \gg 1$, we find

$$u(\rho) = A\,\rho^3 + \tfrac{1}{450\pi^2}\,A^{-1}\,\rho^{-2} + \dots\,, \tag{3.6}$$

(and similarly for $N \neq 1$), where the dots denote subleading terms in ρ and the constant $A > 0$ has to be fixed appropriately, in a way similar to λ_1 in (3.5). It would be interesting to study the analyticity properties of the fixed point solutions more deeply, and to contrast it with the analysis of [32] for the sharp cut-off flow. Despite the simple explicit form of the flow, and its explicit solution for large and small fields, it is more efficient to identify the scaling solution and the related critical exponents using numerical methods.

C. Scaling potential

We have solved the resulting coupled set of differential equations in $d = 3$ dimensions, for $N = 0, 1, \cdots, 10$ and for truncations up to $n_{\rm trunc} = 20$. We have retained only the solution which has one unstable eigendirection, corresponding to the Wilson-Fisher fixed point. Fig. 1 shows the corresponding scaling potential $u_\star$ in the vicinity of the potential minimum. In Fig. 1, the unusual normalisation of the potential has been chosen only for display purposes. The scaling potential has, for all N, a minimum at non-vanishing field. For this reason, the expansion II has better convergence properties than expansion I.

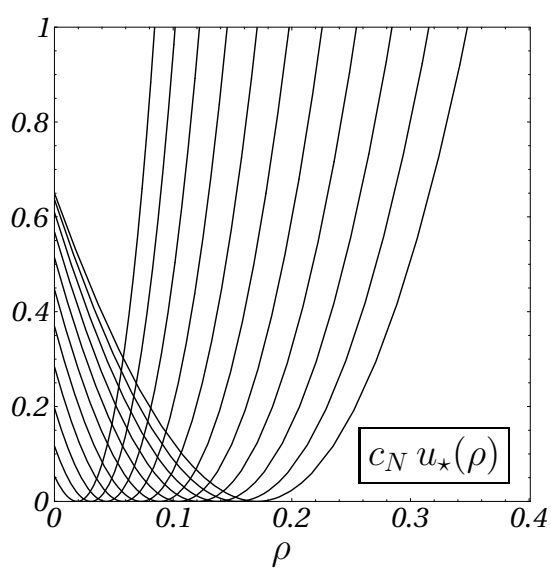

Figure 1: The scaling potential, with $c_N = 40 - 2N$. From left to right: $N = 0, 1, \cdots, 10$.

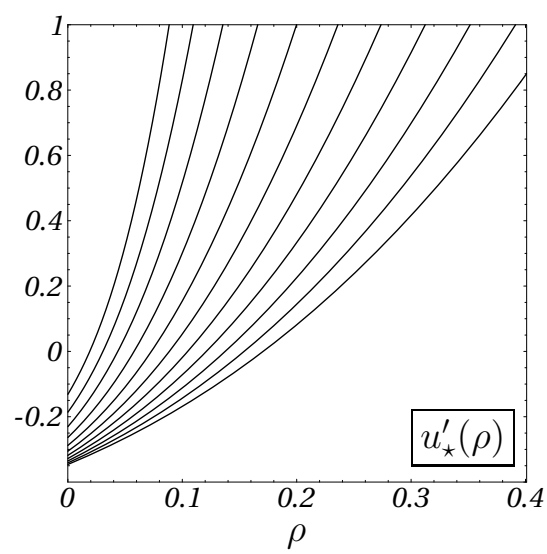

Figure 2: The amplitude $u'_\star(\rho)$ of the scaling solution. From left to right: $N = 0, 1, \cdots, 10$.

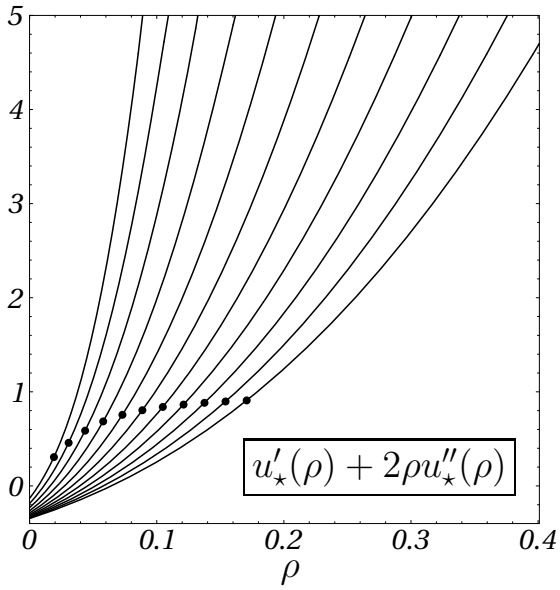

Figure 3: The amplitude $u'_\star + 2\rho u''_\star$ of the scaling solution. The dots indicate the points where $u'_\star = 0$. From left to right: $N = 0, 1, \cdots, 10$.

Fig. 2 shows the amplitude u' at the fixed point. It is a monotonic function of the field. It approaches its most negative values at vanishing field. The flow equation would have a pole at points where $1 + u'$ vanishes. This is, however, never the case, because $1 + u'$ stays always positive. Fig. 3 shows the radial mode of the scaling potential $u'_\star + 2\rho u''_\star$ in the vicinity of the potential minimum. It is a monotonic function of the fields. The dots in Fig. 3 indicate where the derivative $u'_\star$ changes sign. Again, the most negative value is attained at vanishing field and decreases with increasing N, but it stays always above the pole of the flow equation, $1 + u'_\star + 2\rho u''_\star > 0$.

The scaling solution is non-universal. However, critical exponents or the eigenvalues of small perturbations about the scaling solutions *are* universal. For their determination, it is sufficient to study the flow of small perturbations in the vicinity of the scaling potential, which is done next.

IV. CRITICAL EXPONENTS

In this section, we compute the critical exponents to leading order in the derivative expansion. Numerical results are given up to six significant figures (Tab. 1). A higher precision can be achieved, but is not required at the present state. We find a rapid convergence of the polynomial approximation, for all observables considered. Our results are compared with those from other regulators.

A. Eigenvalues

Given the Wilson-Fisher fixed point solution, we can seek for universal critical exponents. In the vicinity of the non-trivial fixed point, we have to solve the eigenvalue equation

$$\partial_t \; \delta u^{(m)} = \omega \, \delta u^{(m)} \tag{4.1}$$

in order to determine the various universal eigenvalues ω. Using the flow equation, setting $d = 3$ and choosing $m = 1$, and expanding the flow to leading order about the Wilson-Fisher fixed point, we find

$$\begin{aligned} 0 = & \left[\omega + 2 - \frac{N}{6\pi^2} \frac{u''_\star}{(1+u'_\star)^2}\right] \delta u' + \frac{1}{3\pi^2} \left[\frac{2N}{1+u'_\star} - \frac{1+u'_\star - \rho u''_\star - 2\rho^2 u'''_\star}{(1+u'_\star + 2\rho u''_\star)^2}\right] \delta u'' \\ & + \frac{1}{3\pi^2} \frac{\rho}{1+u'_\star + 2\rho u''_\star} \, \delta u''' \, . \end{aligned} \tag{4.2}$$

Instead of solving Eq. (4.2) directly for an eigenperturbation $\delta u'$ with eigenvalue ω, we follow a slightly different line which is numerically less demanding. Based on the polynomial expansion used in the previous section, the fixed point potential is given by the set of couplings $\{\lambda_{n,\star}\}$. At the fixed point, the flow of the couplings $\partial_t \lambda_n \equiv \beta_n$ vanishes, $\beta_n(\lambda_{i,\star}) = 0$. The eigenvalues ω of the stability matrix at criticality

$$M_{ij} = \partial \beta_i / \partial \lambda_j |_{\lambda = \lambda_\star} \tag{4.3}$$

correspond to the eigenvalues of Eq. (4.1). Hence, the problem of finding the eigenvalues of Eq. (4.1) reduces to the problem of finding the eigenvalues of the stability matrix M.

N	ν	ω	ω_2	ω_3	ω_4
0	0.592083	0.65788	3.308	6.16	9.2
1	0.649562	0.655746	3.180	5.912	8.80
2	0.708211	0.671221	3.0714	5.679	8.440
3	0.761123	0.699837	2.9914	5.482	8.125
4	0.804348	0.733753	2.9399	5.330	7.867
5	0.837741	0.766735	2.9108	5.2195	7.665
6	0.863076	0.795815	2.8967	5.1409	7.512
7	0.882389	0.820316	2.8916	5.0863	7.396
8	0.897338	0.840612	2.89163	5.04848	7.3086
9	0.909128	0.857384	2.89438	5.02232	7.2425
10	0.918605	0.871311	2.89846	5.00420	7.1921
∞	1	1	3	5	7

Table 1: The first five eigenvalues $\omega_0 < 0 < \omega_1 < \omega_2 < \omega_3 < \omega_4$, with $\nu = -1/\omega_0 > 0$ for various N and $d = 3$ dimensions.

B. Results

We have computed the eigenvalues of (4.3) as functions of the order of the polynomial truncation. The numerical results for the first five eigenvalues for various N and $d = 3$ dimensions are given in Tab. 1 and in Figs. 4 – 8. Results for other regulators are compared in [10] (see also Sects. IV D and V), and results for the asymmetric corrections to scaling are given elsewhere. Exact results, independent on the regularisation, are known for $N = \infty$. The exact eigenvalues are given by $\omega_n = 2n-1+\mathcal{O}(1/N)$, and only the subleading corrections $\mathcal{O}(1/N)$ depend on the regulator. For $N = -2$, it is known that $\nu = \frac{1}{2}$. Tab. 1 shows the first five eigenvalues, ordered as $\omega_0 < 0 < \omega < \omega_2 < \omega_3 < \omega_4$. The critical exponent ν is given by $\nu = -1/\omega_0 > 0$. As a function of N, the eigenvalue ν interpolates monotonically between the exact values $\nu = \frac{1}{2}$ for $N = -2$ and $\nu = 1$ for $N = \infty$. The eigenvalues ω and ω_2 are non-monotonic functions of N. For small N, ω decreases until $N \approx 1$, and increases towards the exact asymptotic value $\omega = 1$ for $N \to \infty$. The eigenvalue ω_2 decreases until $N \approx 7 - 8$ before settling to the asymptotic value $\omega_2 = 3$ at $N = \infty$. The eigenvalues ω_3 and ω_4 are monotonically decreasing functions of N.

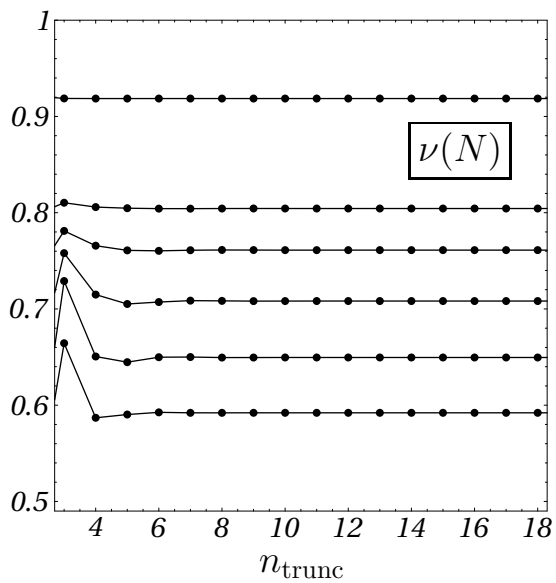

Figure 4: The exponent $\nu(N)$ as a function of N and of the order of the truncation. From top to bottom: $N = 10, 4, 3, 2, 1, 0$.

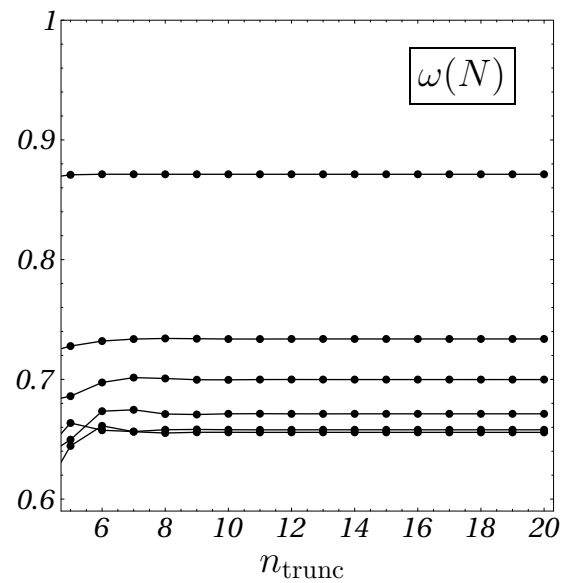

Figure 5: The eigenvalue $\omega(N)$ as a function of N and of the order of the truncation. From top to bottom: $N = 10, 4, 3, 2, 0, 1$.

Fig. 4 shows the results for ν as a function of $n_{\rm trunc}$ and N. It is seen that the expansion is very stable. It convergences already within low order of the truncation towards the asymptotic value. Typically, $n_{\rm trunc} \approx 6$ gives the correct result below the percent level. Furthermore, the convergence is better for larger values of N. This behaviour is observed for all eigenvalues (e.g. Figs. 4 – 8). Fig. 5 shows the same behaviour for the smallest subleading eigenvalue ω. For $n_{\rm trunc} \approx 8$, it has settled below the percent level of the correct result.

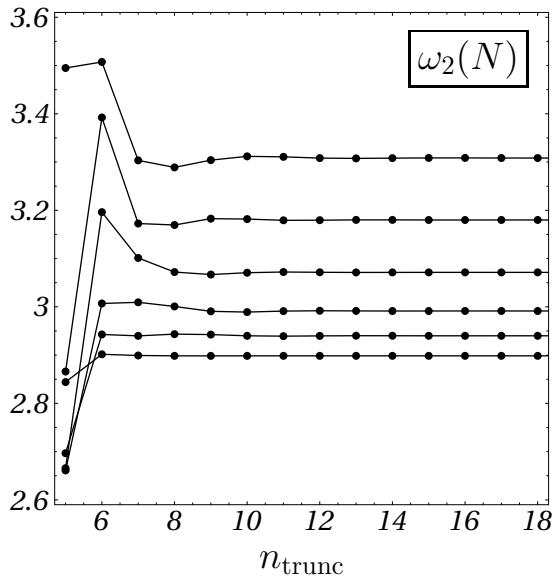

Figure 6: The critical index $\omega_2(N)$ as a function of N and of the order of the truncation. From top to bottom: $N = 0, 1, 2, 3, 4, 10$.

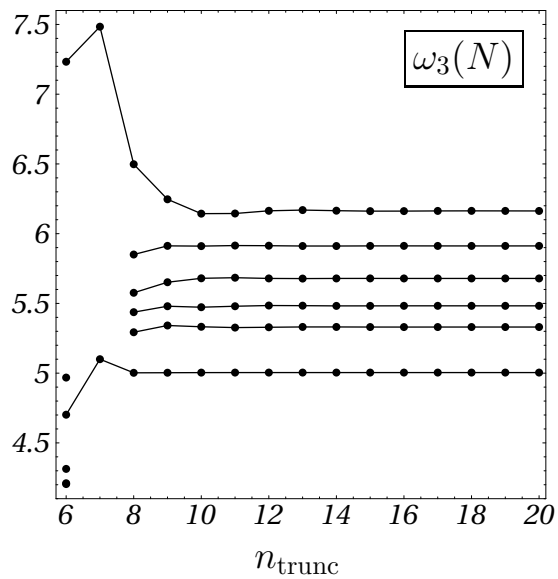

Figure 7: The critical index $\omega_3(N)$ as a function of N and of the order of the truncation. From top to bottom: $N = 0, 1, 2, 3, 4, 10$.

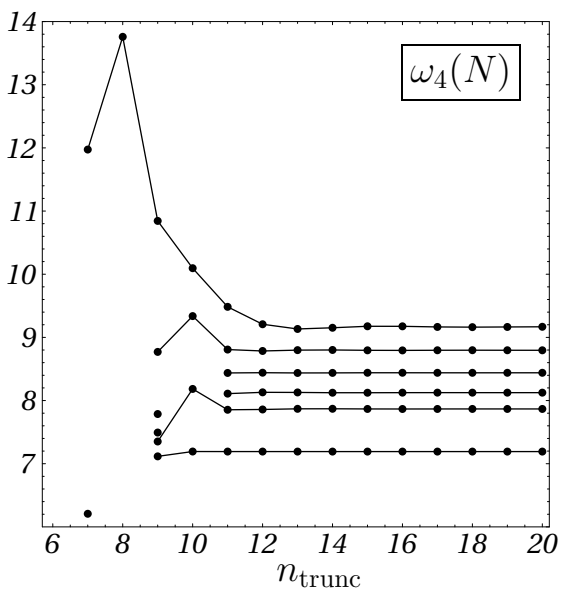

Figure 8: The critical index $\omega_4(N)$ as a function of N and of the order of the truncation. From top to bottom: $N = 0, 1, 2, 3, 4, 10$. The isolated point at $n = 7$ corresponds to $N = 10$, and the two at $n = 9$ to $N = 2$ (upper) and $N = 3$ (lower). The intermediate points (at $n = 8$ and $n = 10$, resp.) are missing because they have a small imaginary part.

For low orders of the truncation, the eigenvalues ω_2, ω_3 and ω_4 (Figs. 6, 7 and 8, respectively) depend more strongly on $n_{\rm trunc}$, and do not even lead to real eigenvalues in some cases (c.f. Figs. 7 and 8). Again, the dependence is even stronger for smaller N. For sufficiently high order in the truncation, however, all eigenvalues are real, and the convergence towards the asymptotic value is fast. Typically, ω_2, ω_3 and ω_4 reach their asymptotic values below the percent level for $n_{\rm trunc} \approx 10, 12$ and 14.

For all eigenvalues, the basic picture is the same: for small $n_{\rm trunc}$, the truncation tends to overshoot the asymptotic value, but with increasing $n_{\rm trunc}$ it relaxes towards it with a

remaining oscillation and decreasing amplitude. From a specific order onwards, the truncation sits – for all technical purposes – on top of the asymptotic value. For a fixed level of accuracy, a lower order in the truncation is required for the dominant observables like ν or ω, while a higher order is required for the subleading eigenvalues. Roughly speaking, to obtain the eigenvalue $\omega_n, n = 0, \cdots$ accurate below the percent level, a truncation with $n_{\rm trunc} \approx 2n + 6$ independent couplings is required.

C. Convergence and stability

Next, we discuss the convergence and stability of the polynomial approximation for an optimised flow. From the results presented so far (cf. Figs. 4 - 8), we conclude that the optimised flow (2.13) leads to a fast convergence of the polynomial approximation for the scaling potential. More importantly, we have seen that the inclusion of further vertex functions — increasing $n_{\rm trunc} \to n_{\rm trunc}+1$ — does not alter the fixed point structure. Rather, it leads to a small modification of the actual fixed point solution and to minor corrections for the critical exponents. This implies that the flow is very stable, and that most of the physical information is already contained in a few leading order terms of the truncation. This result is by no means trivial. A counter example is furnished by the sharp cutoff (see also the following section), where the convergence of the polynomial approximation is poor. Here, the good convergence hinges on the use of an appropriately optimised regulator [7–9].

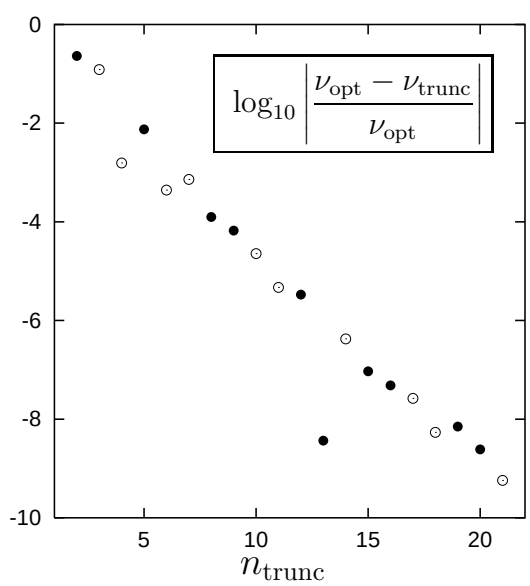

Figure 9: Ising universality class. Convergence of $\nu_{\rm trunc}$ (expansion II) towards $\nu_{\rm opt}$ with increasing truncation. Points where $\nu_{\rm trunc}$ is larger (smaller) than $\nu_{\rm opt}$ are denoted by o (•). Roughly speaking, for $2 < n_{\rm trunc} < 20$, the accuracy of the critical exponents improves by one decimal point every $\Delta n \approx 2 - 2.5$.

Let us have a closer look at the rate of convergence towards the asymptotic values of expansion II (cf. Fig. 9). We denote with $\nu_{\rm trunc}$ the approximate critical exponent which retains $n = n_{\rm trunc}$ independent parameters in the effective action. The semi-logarithmic plot in Fig. 9 then shows the rate with which successive approximations converge towards

the asymptotic value $\nu_{\rm opt}$. The series $\nu_{\rm trunc}$ oscillates about the asymptotical values with a decreasing amplitude and, roughly, a four-fold periodicity in the pattern $++--$. The curve in Fig. 9 can be approximated by a straight line with a slope $\approx -.4$ to $-.5$. Hence, for every $\Delta n \approx 2-2.5$, the accuracy of $\nu_{\rm trunc}$ increases by one decimal place. Here, we have analysed the convergence for $N=1$. For larger N, the convergence is typically faster than for $N=1$, while for $N=0$, it is about the same. Hence, the present considerations are qualitatively the same for all N.

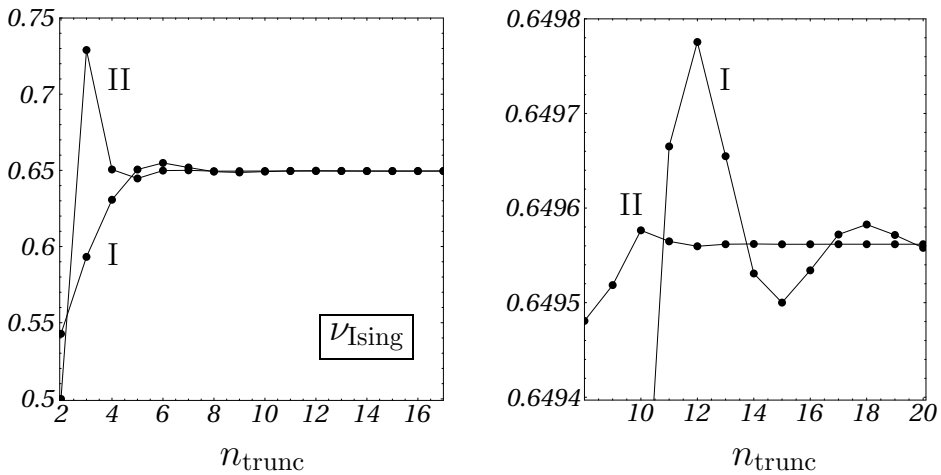

Figure 10: The critical index ν for the Ising universality class as a function of the order of the truncation $n_{\rm trunc}$, for expansion I around vanishing field and expansion II around the non-trivial minimum. Left panel: I and II converge towards the asymptotic value. Right panel: Magnification by a factor of 625. The variation of all data points is below 10^{-3}. II converges faster than I. Expansion I (II) fluctuates about the asymptotic value with decreasing amplitude and a six-fold (four-fold) periodicity; see also Fig. 9.

Until now, we have only employed expansion II, defined in (3.2). It is worthwhile to employ as well expansion I, defined in (3.1). This has been done for the critical exponent ν of the Ising universality class in Fig. 10. The left panel shows that *both* expansions lead to a fast convergence towards the asymptotic value. The right panel is a magnification by 625, showing that expansion II indeed converges faster, although for $n_{\rm trunc}=10$ their difference is already below 10^{-3}. Expansion I fluctuates about the asymptotic value with decreasing amplitude and a six-fold periodicity in the pattern $+++---$.

D. Convergence and scheme dependence

In this section, we discuss the convergence of the ERG flows and the polynomial expansion for various regulators. In Fig. 11, we have computed the critical exponent ν ($N=1$) for the sharp cutoff $r_{\rm sharp}(y) = 1/\,\theta(1-y)-1$, the quartic regulator $r_{\rm quart}(y)=y^{-2}$ and the

optimised regulator (2.12). The left (right) panel uses the expansion I (II). Both $r_{\rm quart}$ and $r_{\rm opt}$ are optimised regulators in the sense coined in section II B. From Fig. 11, three results are noteworthy. First, for the expansion I, we confirm that the convergence is very poor for the sharp cutoff. For both the quartic and the optimised regulator we find a good convergence. Second, the convergence is additionally improved by switching to the expansion II. Third, the critical exponents obey $\nu_{\rm sharp} > \nu_{\rm quart} > \nu_{\rm opt}$. Hence, the better the convergence and the stability of the flow, the smaller the resulting critical exponent ν. This observation is also linked to the convergence of the derivative expansion [10].

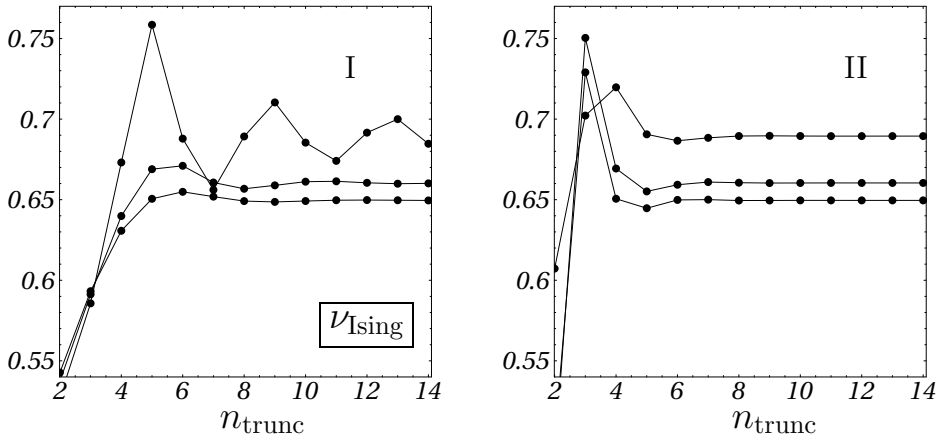

Figure 11: The critical index ν for the Ising universality class. Results are given for Expansion I (left panel) and II (right panel), and for the sharp cutoff (upper curves) the quartic regulator (middle curves) and the optimised regulator (lower curves).

In [7], it has been shown that the gap C (the radius of convergence for amplitude expansions) is linked to the radius of convergence C' for the expansions (3.1) and (3.2). An alternative way for identifying C' consists in studying the complex structure of the scaling solution. For real ρ, the scaling solution is finite and real for all $\rho < \infty$. In the complex plane, the scaling solution has (various) poles. Those closest to the chosen expansion point constrain the radius of convergence C'. For the sharp cutoff and the expansion I, this has been analysed in [32] for $N = 1$. It was found that $\nu_{\rm sharp}$ cannot be determined to an accuracy better than $8 \cdot 10^{-3}$. Hence, the polynomial expansion I for a sharp cutoff does not converge beyond a certain level.

However, the findings of [32] do not imply that polynomial truncations are not trustworthy *per se*. To the contrary, the decisive difference between "good" or "bad" convergence properties stems essentially from an appropriate choice of the regularisation. When optimised, the regularisation implies a significant improvement for either expansion. In this light, the non-convergence of the sharp cutoff flow within expansion I is understood as a

deficiency of the sharp cutoff regularisation. This picture is consistent with the results of [33], who showed that expansion II leads to an improved convergence over expansion I — even for the sharp cutoff.

V. BOUNDS ON CRITICAL EXPONENTS

In this section, we discuss how the critical exponents computed in the previous sections, depend on the regularisation. This discussion is mandatory because observables computed from a truncated flow, are known to depend spuriously on the regularisation. It is decisive to understand the range over which ν_{ERG} may vary as a function of the IR regulator. The origin of the spurious RS dependence is easily understood. The regulator, while regulating the flow, also modifies the coupling amongst all vertex functions of the theory. These regulator induced contributions are of no relevance for the integrated full flow, but they do matter for approximated flows, like in the present case. It is argued that the smallest value for the exponent ν_{ERG} is obtained for the optimised regulator R_{opt}. Prior to this, we recall the results obtained previously in the literature, where, by a number of groups [13,32,20,22,24,10], critical exponents have been computed based on (2.1) for different regulators to leading order in the derivative expansion. For all N, all previously published results obey

$$\nu_{\text{sharp}} \geq \nu_{\text{ERG}} \geq \nu_{\text{min}} \,. \tag{5.1}$$

The regulators studied in the literature cover the sharp cutoff and a variety of smooth cutoff (exponential, power-law), and classes of regulators interpolating between the sharp cutoff and specific smooth cutoffs. Most results have been published for the Ising universality class $N = 1$. For any $N \geq 0$, the smallest value ν_{min} obtained in the literature is larger than the value ν_{opt}: $\nu_{\text{min}} > \nu_{\text{opt}}$. For a detailed comparison of critical exponents to leading and subleading order in the derivative expansion, and a comparison to results from other methods and experiment, we refer to Ref. [10].

A. Upper boundary

Now, we turn to a general discussion on the scheme dependence of ν. At first sight, (5.1) suggests that the possible range for ν is bounded from above and from below. Let us assess the two boundaries. We begin by showing that the inequality $\nu_{\text{sharp}} \geq \nu_{\text{ERG}}$ does not hold for generic regulator. Indeed, the upper boundary in (5.1) can be overcome by choosing regulators which lead to a worse convergence than the sharp cutoff. To see this more explicitly, consider a class of regulators discussed in Appendix B. It is given by

$$R_a(q^2) = a\,(k^2 - q^2)\,\theta(k^2 - q^2)\,, \tag{5.2}$$

and is a variant of the optimised regulator (2.11), to which it reduces for $a = 1$. For $a \to \infty$, it corresponds to the sharp cut off. The regulator leads to an effective radius of convergence

$C_a = a$ for $a < 1$, and $C_a = \frac{a}{2a-1}$ for $a \geq 1$. Since $C_a \ll 1$ for $a \ll 1$, we expect that the corresponding critical exponents will become large. Our results for R_a in (5.2) are given in Fig. 12 (for more details, see Appendix B and Tab. 3). We find that ν_a is a monotonously increasing function for decreasing $a \leq 1$. In particular, for small a we find indeed that $\nu_a > \nu_{\text{sharp}}$. Hence, this result confirms the above picture: Flows with a poor radius of convergence lead to large numerical values for ν.

γ	$\frac{1}{2}$	$\frac{3}{4}$	$\frac{4}{5}$	$\frac{5}{6}$	1	$\frac{3}{2}$	2
ν_γ	1	.7354	.7216	.7142	.6895	.6604	.6496

Table 2: Critical exponents ν (Ising universality class) for the flows ℓ_γ and various γ.

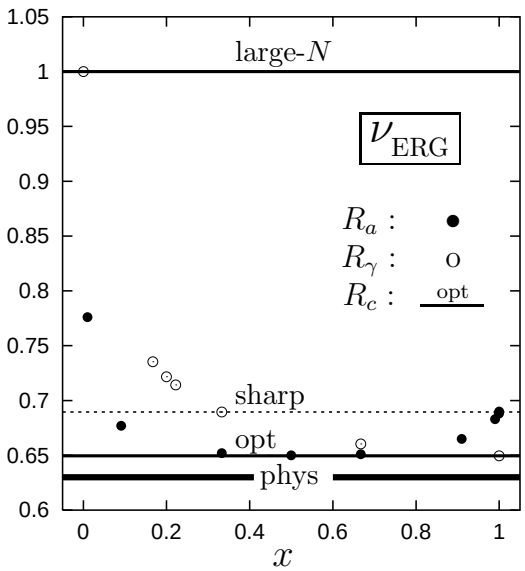

Figure 12: Ising universality class. The critical exponent ν for various classes of regulators. For display purposes, we use $x = \frac{2}{3}(\gamma - \frac{1}{2})$ for R_γ, $x = \frac{a}{a+1}$ for R_a and $x \equiv c$ for R_c. Boundaries: The full line (opt) corresponds to R_c and denotes the lower boundary, the upper full line (large-N) denotes the upper boundary. For comparison: The dashed line (sharp) indicates the sharp cut off value, and the thick full line (phys) the physical value.

Next, we turn to a class of regulators aimed at probing the maximal spread of flows. We recall that, to leading order in the derivative expansion, all regulator-dependence is contained in the functions $\ell(\omega)$. In Ref. [24], it has been shown that the function $\ell(\omega)$ decays at most as ω^{-1}, if the regulator, obeying the basic constraints (2.2)-(2.4), is not a strongly oscillating function of momenta. Hence, regulators leading to a function

$$\ell_\gamma(\omega) \sim (1+\omega)^{1-\gamma} \tag{5.3}$$

define for $\gamma = 2$ a boundary in the space of regulators. This is the case for R_{opt}. No regulator can be found such that $\gamma > 2$ [24]. The proportionality constant in (5.3) is irrelevant because it can be scaled away into the fields in (2.7). The second boundary is set by a mass term regulator $R_{\text{mass}} = k^2$: For a mass term, the corresponding flow is a Callan-Symanzik flow which is not a Wilsonian flow in the strict sense. This comes about because the condition

(2.3) does no longer hold true for $R_{\rm mass}$ in the limit $q^2 \to \infty$. In higher dimensions, this may lead to an insufficiency in the integrating-out of large momentum modes. Inserting $R_{\rm mass}$ into (2.8) in $d = 3$ dimensions leads to (5.3) with $\gamma = \frac{1}{2}$. This sets the second boundary. The regulator R_γ is explicitly known for the cases $\gamma = 2, \frac{3}{2}, 1$ and $\frac{1}{2}$, and corresponds, respectively, to the optimised regulator, the quartic regulator $R_{\rm quart} = k^4/q^2$, the sharp cutoff and a mass term regulator $R_{\rm mass} = k^2$. For all other values of $\gamma \in [\frac{1}{2}, 2]$, R_γ can be recovered explicitly from $\ell_\gamma(\omega)$ [24]. In the present case, we only need to know that such regulators exist.

We have computed the critical index ν_γ for $\ell_\gamma(\omega)$ with $\gamma \in [\frac{1}{2}, 2]$, and our results are given in Tab. 2. In Fig. 12, the results are denoted by open circles for $x = \frac{2}{3}(\gamma - \frac{1}{2})$. As a result, the function ν_γ increases for decreasing γ, $\nu_\gamma \geq \nu_{\rm opt}$. In particular, once $\gamma < 1$, the results obey $\nu_\gamma > \nu_{\rm sharp}$. When $\gamma \to \frac{1}{2}$, the eigenvalues at criticality approach their large-N values $\nu \to 1$ and $\omega_n \to 2n - 1$ for any N. Note that the large-N limit is exact in that it is independent of the regularisation [10]. The large numerical value for $\nu_{\gamma=1/2}$ is due to the deficiencies of the Callan-Symanzik flow. We conjecture that the large-N limit $\nu_{\text{large } N}$ corresponds, for any N, to an upper boundary for any regulator

$$\nu_{\rm ERG} \leq \nu_{\text{large } N} = 1\,. \tag{5.4}$$

B. Lower boundary

Next, we assess the lower boundary. It would be important to know whether the optimised regulator leads to the smallest attainable value for ν in the present approximation. We are not aware of a general proof for this statement. However, strong evidence is provided by studying alterations of the optimised regulator. We have done so for various classes of regulators, three of which are discussed here more explicitly. For more details, we defer to the Appendices B and C. In Appendix B, we employ variants of the optimised regulator, given by the class R_a of (5.2), and by the class R_b defined as

$$R_b(q^2) = (k^2 - q^2)\,\theta(k^2 - q^2)\,\theta(q^2 - \tfrac{1}{2}k^2) + (bk^2 + (1-2b)q^2)\,\theta(\tfrac{1}{2}k^2 - q^2)\,. \tag{5.5}$$

for $0 \leq b \leq \infty$. This class contains the optimised regulator (2.11) for $b = 1$. The limit $b \to \infty$ corresponds to a variant of the standard sharp cutoff. Another new class of regulators R_c is studied in Appendix C, where we allow for an additional k-dependence on a mass scale within the regulator. We use the class

$$R_c(q^2) = (k^2 - q^2 - c\,m_k^2)\,\theta(k^2 - q^2 - c\,m_k^2)\,. \tag{5.6}$$

Here, c is a free parameter and $m_k^2 = U_k''(\phi = 0)$ is the mass term at vanishing field. For $c = 0$, it turns into the optimised regulator (2.11). Due to the implicit scale dependence of

m_k on k, the corresponding flow equations are substantially different from the usual one. Most notably, they contain terms proportional to the flow of m_k.

The classes R_γ, R_a, R_b and R_c probe "orthogonal" directions in the space of regulators. R_γ is sensitive to the analyticity structure of the flow, R_a and R_b are sensitive to alterations of the function $r(y)$ in the low momentum regime, and R_c, while keeping the shape of the regulator $r(y)$ fixed, alters the implicit modifications due to an additional running mass term. As such, R_a, R_b and R_c can be seen as variants of the optimised regulator. The class R_γ covers the largest domain of qualitatively different flows [27].

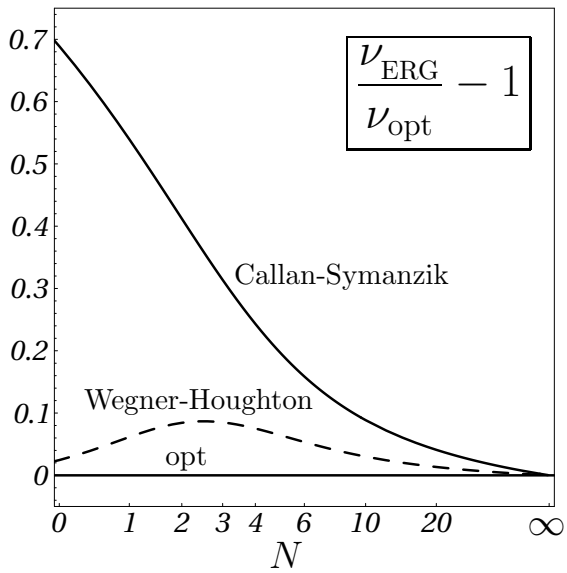

Figure 13: The spread of the critical exponent ν for various N to leading order in the derivative expansion. The upper bound is set by the large-N limit (Callan-Symanzik flow). The sharp cut-off results (Wegner-Houghton flow) are given for comparison.

We have computed the critical exponent ν for the Ising universality class for all these classes of regulators. A part of our results for $N = 1$ is displayed in Fig. 12. Similar results are found for all N. The classical (mean field) value for ν is $\nu_{\rm mf} = \frac{1}{2}$. The results for R_a in (5.2) are displayed in Fig. 12 by full circles, with $x = \frac{a}{a+1}$. Some numerical values are collected in Tab. 3 (cf. Appendix B). It is found that all critical indices ν_a obey $\nu_{\text{large } N} \geq \nu_a \geq \nu_{\rm opt} > \nu_{\rm mf}$. This proves that alterations of the regulator in the low momentum region do not lead to values for ν smaller than $\nu_{\rm opt}$. An analogous result is found for all regulators R_b in (5.5), where $\nu_{\text{large } N} \geq \nu_b \geq \nu_{\rm opt}$. Some numerical values are given in Tab. 4 (Appendix B). In Fig. 12, our results for R_b are represented by open circles, and those for R_c by a dashed line, with $x \equiv c$. All regulators R_c from Eq. (5.6) lead to the *same* critical exponent as $R_{\rm opt}$ in Eq. (2.11), $\nu_c \equiv \nu_{\rm opt}$ (see Appendix C).

In Fig. 13, we discuss the spread of $\nu_{\rm ERG}$ to leading order in the derivative expansion for all $N \geq 0$. The spread $\nu_{\text{large } N}/\nu_{\rm opt} - 1$ is a N-dependent quantity. For $N = 1$, the spread is about 0.54, and hence quite large. For comparison, the relative width with respect to the

sharp cut off $\nu_{\rm sharp}/\nu_{\rm opt} - 1$ is roughly 0.06 and significantly smaller. With increasing N, the spread vanishes as $\sim 1/N$. This follows trivially from the fact that the ERG flow, to leading order in the derivative expansion, becomes exact in the large-N limit [10].

In summary, the critical exponent ν, as a function of the infrared regularisation, is bounded. The upper boundary is realised for flows with a mass term regulator, e.g. Callan-Symanzik flows. The lower boundary is given by

$$\nu_{\rm ERG} \geq \nu_{\rm opt} \tag{5.7}$$

to leading order in the derivative expansion. Hence, $\nu_{\rm opt}$ appears indeed to be the smallest value attainable within the present approximation. The inequality (5.7) provides a quantitative basis for the optimisation procedure which has lead to $R_{\rm opt}$ in the first place. For the observable ν, we have equally shown that the optimised regulator corresponds, at least, to a "local minimum" in the space of all regularisations. Furthermore, we have established flat directions in the space of regulators. Based on the conceptual reasons which have lead to $R_{\rm opt}$ [7,8], we expect that $\nu_{\rm opt}$ even corresponds to the global minimum. At present, however, we have no regulator-independent proof for this conjecture.

VI. DISCUSSION AND CONCLUSIONS

We studied in detail $O(N)$ symmetric scalar theories at criticality, using the ERG method to leading order in the derivative expansion. This included a complete investigation of the Gaussian fixed point in $d > 2$ for arbitrary regulator, and the computation of universal critical exponents and subleading corrections at the Wilson-Fisher fixed point for $d = 3$. Furthermore, we studied the spurious scheme dependence for the critical exponent ν at the Wilson-Fisher fixed point in three dimensions. One of the main new results is that the leading critical exponent, as a function of the IR regulator, is bounded from above and from below as

$$\nu_{\rm opt} \leq \nu_{\rm ERG} \leq \nu_{\rm large\, N}\,. \tag{6.1}$$

This result has been achieved by studying the maximal domain of ERG flows in the present approximation, ranging from Callan-Symanzik flows to optimised flows and variants thereof. The qualitative result – the existence of a non-trivial Wilson-Fisher fixed point – is very stable, although the spread of values for ν is fairly large (see Fig. 13). Supposedly, this is a consequence of a small anomalous dimension η, which constrains higher order corrections. The spread would shrink to zero only to sufficiently high order in the derivative expansion or in the large-N limit.

The important quantitative question is: Which value for ν could be considered as a good approximation to the physical theory? In view of the regulator dependence, a prediction

solely based on (6.1) is of little use. Our answer to this problem is entirely based upon the structure of the ERG flow. We proposed to use specific regulators which lead to more stable ERG flows in the space of all action functionals. The numerical determination of critical exponents and subleading corrections to scaling as given in Tab. 1, is based on an optimised flow. We expect that the results should be in the vicinity of the physical theory. In the present approximation, the results for $\nu_{\rm opt}$ are indeed closest to the physical ones [1],

$$\nu_{\rm phys} < \nu_{\rm opt} \, . \tag{6.2}$$

The understanding of the spurious scheme dependence reduced the ambiguity in ν to a small range about $\nu_{\rm opt}$. Typically, the results from optimised flows other than $R_{\rm opt}$ are close to the values achieved by $R_{\rm opt}$, and hence close to the lower boundary of (6.1). In this light, optimised flows are solutions to a "minimum sensitivity condition" in the space of all IR regularisations [9].

Next we turn to the Callan-Symanzik flow, which is the flow with a mass term regulator $R_{\rm mass} = k^2$. We argued that it defines the upper boundary of values for ν. It is quite remarkable that this flow, for any N, leads to the same eigenvalues at criticality given by the large-N result. Here, this result has been achieved numerically. It would be helpful if it could also be understood analytically. The large numerical value for ν reflects the poor convergence properties of a Callan-Symanzik flow, essentially due to deficiencies in the integrating-out of large momentum modes.

Now we discuss our results concerning polynomial approximations. The reliability of this additional truncation is guaranteed if the approximation convergences reasonably fast. Here, we have established that optimised flows converge very rapidly within the local potential approximation. The efficiency is remarkable: a simple approximation with only six independent operators — say, the running v.e.v. and five running vertex functions up to $(\phi^a\phi_a)^5$ — reproduces the physical result for the exponent ν at the percent level. A better agreement cannot be expected, given that anomalous dimensions of the order of a few percent have been neglected. These findings are in contrast to earlier computations based on the sharp cut-off, where the polynomial approximation has lead to spurious fixed point solutions, even to high order in the approximation [14]. Hence, the efficiency of the formalism not only depends on the choice for the degrees of freedom and the truncation, but additionally, and strongly, on the IR regulator. We conclude that polynomial approximations are reliable for all technical purposes, and even to low orders, if they are backed-up by appropriate regulators. These considerations should be useful in more complex theories whose algebraic complexity requires polynomial approximations, e.g. quantum gravity.

It would be interesting to apply the present ideas to theories like QCD, where the propagating modes are strongly modified in the low momentum regime due to confinement [36,37]. Then, an optimised regulator is found by requiring that the regularised inverse propagator is again flat, i. e. momentum-independent for small momenta. Interesting choices

are $R = (k^2 - X)\,\theta(k^2 - X)$ and $X = \Gamma_k^{(2)}[\phi = \phi_0]$ and variants thereof. Here ϕ_0 denotes a non-propagating background field. This conjecture is supported by first results.

Acknowledgments: I thank J.M. Pawlowski for useful discussions and comments on the manuscript. This work has been supported by the European Community through the Marie-Curie fellowship HPMF-CT-1999-00404.

A. GAUSSIAN FIXED POINT

In this appendix, we discuss the Gaussian fixed point of the flow equation (2.13) in $d > 2$ dimensions and for arbitrary regulator. The Gaussian fixed point corresponds to the specific solution $u_\star(\rho) = \text{const}$. All higher derivatives of the potential vanish, $u_\star^{(n)}(\rho) = 0$. From the flow equation, we deduce that

$$u_\star = \frac{2v_d}{d} N \int_0^\infty dy\, y^{\frac{d}{2}-1} \frac{-r'(y)}{1 + r(y)}\,. \tag{A.1}$$

For the optimised regulator, we find $u_\star = 4Nv_d/d^2$. More information can be extracted by studying small perturbations $\delta u^{(m)}$ around the m-th derivative of the scaling solution $u_\star(\rho)^{(m)}$. The eigenperturbations obey the differential equation

$$\partial_t\, \delta u^{(m)} = \omega\, \delta u^{(m)} \tag{A.2}$$

with eigenvalues ω. Expanding the flow equation to leading order in δu, the eigenvalues obey

$$0 = [\omega + d - (d-2)m]\; \delta u^{(m)} + \left[2A(\frac{N}{2} + m) - (d-2)\rho\right]\; \delta u^{(m+1)} + 2\rho A\, \delta u^{(m+2)}\,. \tag{A.3}$$

Here, the scheme-dependent coefficient A is given by

$$A = 2v_d \int_0^\infty dy\, y^{\frac{d}{2}-3} \frac{-r'(y)}{[1 + r(y)]^2} \tag{A.4}$$

and $0 < A < \infty$. For the optimised regulator, $A_{\text{opt}} = 4v_d/d$. Introducing new variables $x = (d-2)\rho/(2A)$ and $f(x) = \delta u(\rho)$, the differential equation (A.3) transforms into the (generalised) Laguerre differential equation

$$0 = \left(\frac{d+\omega}{d-2} - m\right) f^{(m)}(x) + \left(\frac{N}{2} + m - x\right) f^{(m+1)}(x) + x f^{(m+2)}(x)\,. \tag{A.5}$$

We consider only polynomial solutions to Eq. (A.5). The requirement that solutions to Eq. (A.5) are bounded by polynomials fixes the possible eigenvalues as

$$\omega = (d-2)(n+m) - d \tag{A.6}$$

for non-negative integers n and m. Apart from an irrelevant normalisation constant, the n-th eigensolution to Eq. (A.5) are given by the (generalised) Laguerre polynomials

$$\delta u^{(m)}(\rho) = L_n^{m-1+N/2}\left(\frac{2A\,\rho}{d-2}\right) . \tag{A.7}$$

Eq. (A.7) is the most general eigensolution at the Gaussian fixed point in $d > 2$ dimensions with eigenvalues given by Eq. (A.6). The result holds for arbitrary regulator function. The scheme dependence enters only the argument of the Laguerre polynomials in Eq. (A.7). It is interesting to note that the eigenvalues are independent of the regularisation scheme. Furthermore, the rescaled differential equation (A.5) is also independent of the regulator.

In $d = 3$ dimensions, the relevant and marginal operators are $L_0^{N/2-1}$, $L_1^{N/2-1}$, $L_2^{N/2-1}$ and $L_3^{N/2-1}$ with eigenvalues $\omega = -3, -2, -1$ and 0 for $m = 0$, or $L_0^{N/2}$, $L_1^{N/2}$ and $L_2^{N/2}$ with eigenvalues $\omega = -2, -1$ and 0 for $m = 1$. In $d = 4$ dimensions, the relevant and marginal operators are $L_0^{N/2-1}$, $L_1^{N/2-1}$ and $L_2^{N/2-1}$ with eigenvalues $\omega = -4, -2$ and 0 for $m = 0$, or $L_0^{N/2}$ and $L_1^{N/2}$ with eigenvalues $\omega = -2$ and 0 for $m = 1$. For $m \geq \frac{d}{d-2}$, all eigenoperators are marginal or irrelevant.

For $2m + N = 1$ ($2m + N = 3$), the solution Eq. (A.7) can be rewritten in terms of Hermite polynomials of even (odd) degree,

$$m = \tfrac{1-N}{2}: \quad \delta u^{(m)}(\rho) = \frac{(-1)^n}{n!}\, 2^{-2n}\, H_{2n}\left(\sqrt{\frac{2A\rho}{d-2}}\right) \tag{A.8}$$

$$m = \tfrac{3-N}{2}: \quad \delta u^{(m)}(\rho) = \frac{(-1)^n}{n!}\, 2^{-2n-1} \sqrt{\frac{d-2}{2A\rho}}\, H_{2n+1}\left(\sqrt{\frac{2A\rho}{d-2}}\right) . \tag{A.9}$$

Let us finally mention that some of these solutions have been given earlier in the literature for the case of a sharp cutoff regulator (with $A_{\text{sharp}} = 1$): for $N = 1$ and $m = 1$, Eq. (A.9) has been given in Ref. [13], and Eq. (A.7) for $m = 1$ has been given in Ref. [20].

B. VARIANTS OF THE OPTIMISED CUTOFF

In this appendix, we discuss variants of the optimised regulator (2.11). The aim is to probe whether certain alterations of the regulator may lead to lower values for the critical exponent ν. Here, the properties of the regularisation are changed in the low momentum region by modifying the function $r(y)$. In the following appendix, we discuss modifications of $r(y)$ through the introduction of additional (theory-dependent) k dependent parameters.

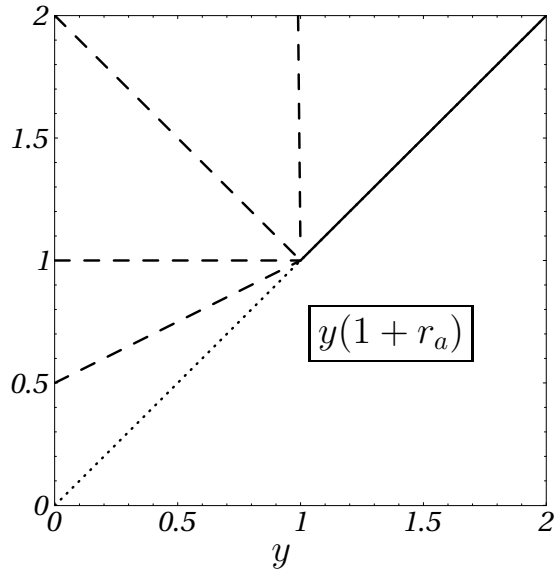

Figure 14: The function $y(1+r_a)$ for the class of regulators (B.1). All lines for different a coincide for large momenta $y \in [1,\infty]$ (full line), but differ for small momenta $y \in [0,1[$ (dashed lines). The dashed lines clock-wise from the bottom: $a = \frac{1}{2}, 1, 2$ and ∞. The short dashed line corresponds to $a = 0$ (no regulator).

1. Definition

In this appendix, we discuss two variants of the optimised regulator (2.11). First, we consider the class of regulators given by

$$R_a(q^2) = a\,(k^2 - q^2)\,\theta(k^2 - q^2)\,. \tag{B.1}$$

These regulators have a compact support. They vanish for all $q^2 > k^2$. In the infrared, they have a mass-like limit $R_a(q^2 \to 0) = ak^2$ for all $0 < a < \infty$. The limit $a \to \infty$ corresponds to the sharp cut-off case. For $a = 0$, the regulator is removed completely. For $a = 1$, the regulator (B.1) reduces to the optimised regulator (2.11). As a function of a, the regulators differ only in the momentum regime $y \in [0,1[$, where $y \equiv q^2/k^2$. The dimensionless functions r_a corresponding to (B.1) are given by

$$r_a(y) = a\,(\tfrac{1}{y} - 1)\,\theta(1 - y)\,. \tag{B.2}$$

In Fig. 1, we have displayed the function $y(1 + r_a)$ for various cases. The full line corresponds to the range $y \in [1,\infty]$, for all regulators (B.1). The dashed lines, clock-wise from the bottom, correspond to $a = \frac{1}{2}, 1, 2$ and ∞. The gaps associated to (B.1) are given by $C_a = \frac{a}{2a-1}$ for $a \geq 1$, and $C_a = a$ for $\frac{1}{2} < a < 1$. They are obtained from the normalised analogue of (B.1), chosen such that $r_a(\frac{1}{2}) = 1$.

Second, we consider another variant of the optimised regulator, where the properties of the regularisation are changed only in the low momentum region by modifying the function $r(y)$. Consider the class of regulators given by

$$R_b(q^2) = (k^2 - q^2)\,\theta(k^2 - q^2)\,\theta(q^2 - \tfrac{1}{2}k^2) + (bk^2 + (1 - 2b)q^2)\,\theta(\tfrac{1}{2}k^2 - q^2)\,. \tag{B.3}$$

These regulators have a compact support. They vanish for all $q^2 > k^2$. In the infrared, they have a mass-like limit $R_b(q^2 \to 0) = b\,k^2$ for all $0 < b < \infty$. At first sight, it may seem that (B.3) is not a viable regulator for $b = 0$, because $R_{b=0}$ vanishes in the infrared limit (no gap). However, for $b = 0$ the function $\partial_t R_{b=0}$ vanishes identically for all $q^2 < \frac{1}{2}k^2$. Hence, (B.3) provides a gap because $R_{b=0}(\frac{1}{2}k^2) = \frac{1}{2}k^2 > 0$. For $b = 1$, the regulator (B.3) reduces to the optimised regulator (2.11). As a function of b, the regulators differ only in the momentum regime $y \in [0, \frac{1}{2}[$, where $y \equiv q^2/k^2$. The dimensionless functions r_b corresponding to (B.3) are given by

$$r_b(y) = (\tfrac{1}{y} - 1)\,\theta(1-y)\,\theta(y - \tfrac{1}{2}) + (\tfrac{b}{y} + 1 - 2b)\,\theta(\tfrac{1}{2} - y)\,. \tag{B.4}$$

In Fig. 15, we have displayed the function $y(1+r_b)$ for various cases. The full line corresponds to the range $y \in [\frac{1}{2}, \infty]$, for all regulators (B.3). The dashed lines, clock-wise from the bottom, correspond to $b = 0, \frac{1}{2}, 1, 2$ and ∞. By construction, the regulator is normalised as $r_b(\frac{1}{2}) = 1$. The associated gaps are given by $C_b = 1$ for $b \geq 1$ and $b = 0$ (see below), and $C_b = b$ for $0 < b < 1$. For comparison, we have also given the curve for the standard sharp cutoff (dotted line). The corresponding gap is $C_{\text{sharp}} = \frac{1}{2}$.

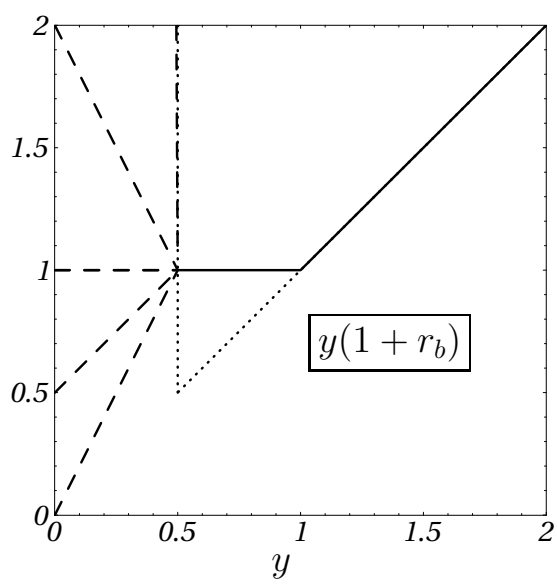

Figure 15: The function $y(1+r_b)$ for the class of regulators (B.3). All lines for different b coincide for large momenta $y \in [\frac{1}{2}, \infty]$ (full line), but differ for small momenta $y \in [0, \frac{1}{2}]$ (dashed lines). The dashed lines clock-wise from the bottom: $b = 0, \frac{1}{2}, 1, 2$ and ∞. The standard sharp cutoff regulator (dotted line) is given for comparison.

The regulators R_a and R_b have a similar low momentum limit for $q^2 \to 0$, e.g. $R_a(q^2 \to 0) = R_{b=a}(q^2 \to 0) = a\,k^2$. The crucial difference between them concerns the intermediate momentum regime $q^2 \approx k^2$. Here, the regulator R_b leads by construction to a plateau for $y(1 + r_b)$, which is absent for R_a.

2. Flows

In order to employ (B.1) for the computation of critical exponents in $d = 3$, the associated flows $\ell(\omega) \to \ell_a(\omega)$ have to be computed. For the function $\ell_a(\omega)$ and for $a \leq 1$, we find in

$d = 3$ (similar expressions are found for any d)

$$\ell_a(\omega) = \frac{2a}{1-a}\left[1 - \sqrt{\frac{a+\omega}{1-a}}\arctan\sqrt{\frac{1-a}{a+\omega}}\right] . \tag{B.5}$$

The region $a > 1$ is obtained by analytical continuation:

$$\ell_a(\omega) = \frac{2a}{1-a}\left[1 - \sqrt{\frac{a+\omega}{a-1}}\operatorname{arctanh}\sqrt{\frac{a-1}{a+\omega}}\right] . \tag{B.6}$$

These flows have the following structure. They have poles on the negative ω-axis at $\omega = -1$. For $a = \infty$, the function decays only logarithmically for asymptotically large ω. In the limiting cases $a = 1$ and ∞, we find

$$\ell_{a=1}(\omega) = \tfrac{2}{3}(1+\omega)^{-1} \tag{B.7}$$

$$\ell_{a=\infty}(\omega) = -\ln(1+\omega) + \text{const.} \tag{B.8}$$

For $a = 1$, in (B.7), both expressions (B.5) and (B.6) have the same limit discussed earlier in [8]. In the limit $a \to \infty$, the resulting regulator is equivalent to the standard sharp cut-off.

In order to employ the regulator R_b from (B.3) for the computation of critical exponents in $d = 3$, the associated flows $\ell(\omega) \to \ell_b(\omega)$ have to be computed. In full analogy to the preceding computation, we find in $d = 3$ (similar expressions are found for any d) for the function $\ell_b(\omega)$ and for $b \leq 1$

$$\ell_b(\omega) = \tfrac{2}{3}(1-2^{-3/2})(1+\omega)^{-1} + \frac{b}{\sqrt{2}(1-b)}\left[1 - \sqrt{\frac{b+\omega}{1-b}}\arctan\sqrt{\frac{1-b}{b+\omega}}\right] . \tag{B.9}$$

The region $b > 1$ is obtained by analytical continuation:

$$\ell_b(\omega) = \tfrac{2}{3}(1-2^{-3/2})(1+\omega)^{-1} + \frac{b}{\sqrt{2}(1-b)}\left[1 - \sqrt{\frac{b+\omega}{b-1}}\operatorname{arctanh}\sqrt{\frac{b-1}{b+\omega}}\right] . \tag{B.10}$$

These flows have the following structure. They have poles on the negative ω-axis at $\omega = -1$ due to the first term on the r.h.s. in (B.9) and (B.10). For large ω and $b < \infty$, both expressions decay as ω^{-1}. For $b = \infty$, the decay is only logarithmic. Let us consider the three limiting cases $a = 0, 1$ and ∞. We find

$$\ell_{b=0}(\omega) = \tfrac{2}{3}(1-2^{-3/2})(1+\omega)^{-1} \tag{B.11}$$

$$\ell_{b=1}(\omega) = \tfrac{2}{3}(1+\omega)^{-1} \tag{B.12}$$

$$\ell_{b=\infty}(\omega) = \tfrac{2}{3}(1-2^{-3/2})(1+\omega)^{-1} - \tfrac{1}{2\sqrt{2}}\ln(1+\omega) + \text{const.} \tag{B.13}$$

For $b = 0$, the momentum regime $q^2 < \frac{1}{2}k^2$ does not contribute to the flow and the effective gap for $b = 0$ is $C_0 = 1$. This is seen directly from (B.9) and (B.11): the first term of

(B.9) stems from the momentum interval $\frac{1}{2}k^2 \leq q^2 \leq k^2$, which is the only term surviving in (B.11). For $b = 1$, in (B.12), both terms of (B.9) combine to the known result discussed earlier in [8]. Finally, we turn to the limit $b \to \infty$. The resulting regulator is similar to the standard sharp cut-off, with, however, an important difference. For the sharp cutoff, the function $y(1 + r_b)$ has no plateau in the momentum regime $\frac{1}{2}k^2 \leq q^2 \leq k^2$ (see Fig. 15), which leads to $\ell_{\text{sharp}}(\omega) = -\ln(1 + \omega)$. In (B.8), the sharp-cutoff-like logarithmic term is clearly seen, and is due to the momentum integration with $y \in [0, \frac{1}{2}]$. However, a decisive difference is the additional term in (B.8). Notice also that the constant in (B.13) is actually infinite, but field independent. Hence, it is irrelevant for a computation of critical exponents (only the functions $\partial_\omega \ell_b(\omega)$ are needed).

3. Results

For R_a, we have computed the critical exponent ν for the Ising universality class using the flow equation (2.7) with (B.5), (B.6) (see Tab. 3). We confirm that $\nu_{a=\infty} = \nu_{\text{sharp}}$ and that $\nu_{a=1} = \nu_{\text{opt}}$. For all $a > 1$ ($a < 1$), ν_a is a monotonically increasing (decreasing) function with increasing a, hence $\nu_a \geq \nu_{\text{opt}}$. Notice that the smallest value for ν is obtained for the largest value for the gap parameter.

a	10^{-2}	10^{-1}	$\frac{1}{2}$	1	2	10	10^2	10^3	10^4	∞
C_a	10^{-2}	10^{-1}	$\frac{1}{2}$	1	$\frac{2}{3}$	$\frac{10}{19}$	$\frac{100}{199}$	$\frac{1000}{1999}$	$\frac{10000}{19999}$	$\frac{1}{2}$
ν_a	.776	.677	.652	.650	.651	.665	.683	.688	.689	.690

Table 3: Critical exponents ν (Ising universality class) for the regulator R_a and various a.

b	0	$\frac{1}{2}$	1	10	100	∞
ν_b	.6495	.6518	.6495	.6594	.6675	.6699

Table 4: Critical exponents ν (Ising universality class) for the flows with R_b and various b.

For R_b, we have also computed the critical exponent ν for the Ising universality class using the flow equation (2.7) with (B.9), (B.10). We find that $\nu_{b=0} = \nu_{b=1} = \nu_{\text{opt}}$. For $b < 1$, we have $\nu_b > \nu_{\text{opt}}$. However, for too small values of b, $1 \gg b > 0$, the regulator leads to a very small gap and the polynomial approximation does no longer converge to a definite result, which is an artifact of the regulator. For $b > 1$, ν_b is a monotonic function of b with $\nu_{b=\infty} \geq \nu_b > \nu_{\text{opt}}$. It is interesting to discuss the case $b = \infty$ in more detail. Here, $\nu_{b=\infty} = .6699\cdots$ which should be compared to $\nu_{\text{sharp}} = .6895\cdots$ and to $\nu_{\text{opt}} = .6495\cdots$. From the structure of the flow, it is clear that the difference $\nu_{\text{sharp}} - \nu_{b=\infty}$ has to be attributed to momenta with $y \in [\frac{1}{2}, 1]$. Hence, the "flattening" of the standard sharp cutoff reduces

the critical exponent by a few percent. On the technical level, this reduction is attributed to the non-logarithmic term in (B.13). However, the smallest value for ν is obtained only in case the logarithmic term is absent, as it happens in both (B.11) and (B.12).

C. CUTOFFS WITH INTRINSIC SCALING

In this appendix, we study regulators with additional intrinsic scale-dependent parameters.

1. Definition

Up to now, we have considered IR regulators $R(q^2)$ which depend on momenta only through the combination q^2/k^2, cf. Eq. (2.5). In Eq. (2.5), the essential IR cutoff is provided by the function $r(q^2/k^2)$, which cuts off the momentum scale q^2 in a way which is independent of the particular theory studied. The k dependence of $R(q^2)$ is the trivial k dependence linked to the dimensionality of R. The situation is different once further k-dependent functions are introduced into the regulator. Typically, this is done by replacing

$$R(q^2) \to R(q^2, \{Z_k, m_k^2, \ldots\})\,. \tag{C.1}$$

Here, the set $\{Z_k, m_k^2, \ldots\}$ denotes scale-dependent parameters of the specific theory studied, like the wave-function renormalisation Z_k or mass parameters m_k. It is expected that the substitution (C.1) leads to an improved convergence and stability of the flow. A well-known example for (C.1) is given by $R(q^2) \to Z_k R(q^2)$, which is often used beyond the leading order in a derivative expansion. Here, the introduction of Z_k in the regulator simplifies the study of scaling solutions. In the context of non-Abelian gauge theories, regulators like Eq. (C.1) have been used in [37] based on the replacement $q^2 \to \bar{\Gamma}_k^{(2)}[\phi_0]$ in the regulator, and hence

$$R(q^2) \to R[\bar{\Gamma}_k^{(2)}]\,. \tag{C.2}$$

Again, this type of regulator has been motivated to stabilise the flow and to encompass possible poles in the flow due to mass terms for the gluonic fields [37]. Notice that $\bar{\Gamma}_k^{(2)}$ in Eq. (C.2) cannot be the full field-dependent functional, because elsewise the flow equation would no longer be the correct one. Instead, one has to evaluate it for some fixed background field $\phi = \phi_0$ (hence the bar on $\bar{\Gamma}_k^{(2)}$). In the present case, and to leading order in the derivative expansion, we have

$$\bar{\Gamma}_k^{(2)}[\phi_0] = q^2 + U_k''(\phi_0)\,. \tag{C.3}$$

Here, $U''(\phi_0)$ corresponds to a scale-dependent effective mass term. Within the non-convex part of the potential, or in a phase with spontaneous symmetry breaking, we have $m_k^2 \equiv$

$U''(\phi_0) < 0$. Hence the regulator Eq. (C.2) is a special case of Eq. (C.1). In the remainder, the optimised regulator (2.12) is used to define a class of regulators of the form (C.1), namely

$$R_c(q^2) = (k^2 - q^2 - c\, m_k^2)\, \theta(k^2 - q^2 - c\, m_k^2)\,. \tag{C.4}$$

Hence, $R_c(q^2) = R_{\rm opt}(q^2 + c\, m_k^2)$. Effectively, this corresponds to the replacement $k^2 \to k^2_{\rm eff}(k) = k^2 + c\, m_k^2$. In terms of $r(y)$ defined in Eq. (2.5), the regulator is given as

$$r_c(y) = (\tfrac{1-c\bar\omega}{y} - 1)\, \theta(1 - y - c\,\bar\omega)\,, \tag{C.5}$$

and the dimensionless mass parameter is

$$\bar\omega \equiv m_k^2/k^2\,. \tag{C.6}$$

Below, we use $m_k^2 \equiv U''(\phi_0 = 0)$. The regulator (C.4) can be seen as a 'sliding' cutoff, because at any scale k, only the k-dependent momentum interval $y \in [0, 1 - c\,\bar\omega_k]$ contributes to the flow. For $c = 0$, the regulator reduces to (2.11), while for $c = 1$ it turns into a regulator of the form (C.2) with (C.3). Due to the additional dependence on m_k^2/k^2, the structure of the flow equation is now different.

2. Flows

Let us compute the flow for the regulator Eq. (C.4). Inserting Eq. (C.4) into Eq. (2.8), and after some straightforward algebra, we find

$$\ell_c(\omega) = \tfrac{2}{d}(1 - c\,\bar\omega)^{d/2}\, \frac{1 - c\,\bar\omega - \frac{c}{2}\partial_t\bar\omega}{1 - c\,\bar\omega + \omega} \tag{C.7}$$

Notice that the function Eq. (C.7) depends now on $\bar\omega$ and on the *flow* of $\bar\omega$. This is generic to regulators of the form (C.1) or (C.2), because the implicit scale dependence of m_k^2 leads to an additional term $\sim \partial_t m_k^2$ in the flow equation. The flow equation (2.7) with Eq. (C.7) becomes

$$\begin{aligned}\partial_t u + du - (d-2)\rho u' = (N-1)(1 - c\,\bar\omega)^{d/2}\, &\frac{1 - c\,\bar\omega - \frac{c}{2}\partial_t\bar\omega}{1 - c\,\bar\omega + u'} \\ + (1 - c\,\bar\omega)^{d/2}\, &\frac{1 - c\,\bar\omega - \frac{c}{2}\partial_t\bar\omega}{1 - c\,\bar\omega + u' + 2\rho u''}\end{aligned} \tag{C.8}$$

Here, in order to simplify the expressions, we have rescaled the irrelevant numerical factor $\frac{4}{d}v_d$ into the fields and the potential. In order to find an explicit form of the flow, the running mass term needs to be specified. We chose $\bar\omega = u'(\rho = 0)$. This choice is motivated by the fact that the function u', on the fixed point, reaches its most negative value at vanishing field. For $c = 0$, the original flow may run into a pole at $u' = -1$. The present choice shifts the pole to $u'(\rho) = -1 + c\, u'(0)$. Since $u'(\rho) - u'(0) \geq 0$ for a scaling solution, the right-hand

side of (C.8) has no longer an explicit pole for $c = 1$. This has been the motivation for the structure of the regulator used in [37]. However, as we shall see, the full flow still has an implicit pole due to the flow of $\bar{\omega}$ in (C.8). In terms of

$$\lambda_0 \equiv u'(\rho = 0)\,, \quad \lambda_1 \equiv u''(\rho = 0)\,, \tag{C.9}$$

and after inserting Eq. (C.7) into Eq. (C.8) and collecting terms proportional to the flow of λ_0, we find

$$\partial_t \lambda_0 = -\frac{2\lambda_0 + \lambda_1(N+2)(1-c\,\lambda_0)^{1+d/2}[1+\lambda_0(1-c)]^{-2}}{1-\frac{1}{2}c\lambda_1(N+2)(1-c\,\lambda_0)^{d/2}[1+\lambda_0(1-c)]^{-2}}\,. \tag{C.10}$$

For the quartic coupling, and suppressing terms proportional to $u'''(0)$, we find

$$\begin{aligned}\partial_t \lambda_1 = -\lambda_1 &\left(4 - d - \lambda_1 \frac{2(N+8)\,(1-c\,\lambda_0)^{d/2}}{[1+(1-c)\lambda_0]^3}\right) \times \\ &\left(1 - c\,\lambda_0 + \frac{c}{2}\frac{\lambda_0 + \frac{\lambda_1}{2}(N+2)\,(1-c\,\lambda_0)^{1+d/2}[1+(1-c)\;\lambda_0]^{-2}}{1 - c\frac{\lambda_1}{2}(N+2)\,(1-c\,\lambda_0)^{d/2}[1+(1-c)\;\lambda_0]^{-2}}\right)\end{aligned} \tag{C.11}$$

The structure of the flows (C.10) and (C.11) is easily understood. The denominator in (C.10) stems from a resummation of the back coupling of $\partial_t \lambda_0$. The denominator becomes trivial for $c = 0$. The numerator contains the usual scaling term and a modified threshold behaviour, which depends now on c. A similar structure appears for the flow of the quartic coupling. Simpler forms of the flow are obtained for $c = 0$ (no back-coupling of a running mass term) or $c = 1$. For $c = 0$, we have

$$\partial_t \lambda_0 = -2\lambda_0 + \lambda_1 \frac{N+2}{(1+\lambda_0)^2}\,, \tag{C.12}$$

$$\partial_t \lambda_1 = -(4-d)\lambda_1 + \lambda_1^2 \frac{2(N+8)}{(1+\lambda_0)^3}\,, \tag{C.13}$$

while for $c = 1$, the result is

$$\partial_t \lambda_0 = -\frac{2\lambda_0 + \lambda_1(N+2)(1-\lambda_0)^{1+d/2}}{1-\frac{1}{2}\lambda_1(N+2)(1-\lambda_0)^{d/2}}\,, \tag{C.14}$$

$$\partial_t \lambda_1 = -\lambda_1(1+\lambda_0)\frac{4 - d - \lambda_1\, 2(N+8)\,(1-\lambda_0)^{d/2}}{1-\frac{1}{2}\lambda_1(N+2)(1-\lambda_0)^{d/2}}\,. \tag{C.15}$$

Hence, (C.12) and (C.13) have a putative pole at $\lambda_0 = -1$. In turn, (C.14) and (C.15) have a putative pole at $(N+2)\lambda_1 = 2(1-\lambda_0)^{-d/2}$. The putative pole is absent for $N = -2$.

3. Results

From the explicit form of the function (C.7), and without having made yet the explicit choice (C.9) for the mass term m_k^2, we conclude that the non-universal fixed point solution $\partial_t u = 0$ of (2.7) for either $R_{\rm opt}$ from (2.11), or the class of regulators R_c from (C.4) are related by a simple rescaling of the fields. The reason is the following: on the fixed point $\partial_t u = 0$, we also have $\partial_t(m_k^2/k^2) = 0$. Hence, the functions Eq. (C.7) do no longer depend on the flow of the mass term. Hence, Eq. (C.7) becomes $\ell(\omega) = \frac{2}{d}C^{d/2+1}/(C+\omega)$, with $C \equiv 1 - c\,\bar{\omega} = \text{const}$ on a fixed point. This function is equivalent to a flow derived from $R_{\rm opt}$. Hence, it suffices to rescale $u \to u/C^{d/2}$ and $\rho \to \rho/C^{d/2+1}$ in order to transform the fixed point solution for arbitrary c onto the fixed point equation for $c = 0$.

Next, we check the c dependence of critical exponents. A priori, the critical exponents are sensitive to the flow in the vicinity of the fixed point, and hence to the additional terms $\partial_t \lambda_0$ in the flow equation. We have solved the flow (C.8) with (C.10) numerically, within the polynomial approximation defined in Eq. (3.1) up to $n_{\rm trunc} = 20$. The eigenvalues at criticality are found to be *independent* on the parameter c. The results correspond to the lower full line in Fig. 12 (and $x \equiv c$). Furthermore, we found that the critical exponents for different c agree for every single order in the truncation. Hence, for $N = 1$, the exponent $\nu_{\rm trunc}$ as obtained from (C.8) with (C.10) are given by the line I in Fig. 10.

In summary, the introduction of scale-dependent parameters into the regulator has lead to a significant change of the flow equations and their pole structure. Hence, the approach to a fixed point solution, and stability properties of the flow are quite different. Here, we studied the replacement $R_{\rm opt}(q^2) \to R_{\rm opt}(q^2 + c\,m_k^2)$. Universal quantities are independent of c, because the modified regulator is linked to the optimised one through the replacement $k^2 \to k^2_{\rm eff}(k) = k^2 + c\,m_k^2$ in the flow equation. This should be irrelevant for universal observables at a fixed point, as has been confirmed explicitly. For the same reason, the entire class of regulators $R_a(q^2 + c\,m_k^2) \equiv a R_{\rm opt}(q^2 + c\,m_k^2)$ leads to c-independent critical exponents. Still, the flows are completely different for different a. Therefore, c can be used as a free parameter to stabilise the flow, without affecting the physical result. If the substitution $R(q^2) \to R(q^2 + c\,m_k^2)$ cannot be rephrased as a redefinition of the infrared scale, it is expected that also universal observables no longer remain insensitive to free parameters like c. This case should be studied separately.

REFERENCES

[1] J. Zinn-Justin, *Quantum Field Theory And Critical Phenomena*, Oxford, Clarendon (1989).

[2] J. Polchinski, Nucl. Phys. **B231** (1984) 269.

[3] C. Wetterich, Phys. Lett. **B301** (1993) 90.

[4] U. Ellwanger, Z. Phys. C **62** (1994) 503 [hep-ph/9308260].

[5] T. R. Morris, Int. J. Mod. Phys. **A9** (1994) 2411 [hep-ph/9308265].

[6] For recent reviews, see:
C. Bagnuls and C. Bervillier, Phys. Rept. **348** (2001) 91 [hep-th/0002034],
J. Berges, N. Tetradis and C. Wetterich, hep-ph/0005122.

[7] D. F. Litim, Phys. Lett. **B486** (2000) 92 [hep-th/0005245].

[8] D. F. Litim, Phys. Rev. D **64** (2001) 105007 [hep-th/0103195].

[9] D. F. Litim, Int. J. Mod. Phys. A **16** (2001) 2081 [hep-th/0104221].

[10] D. F. Litim, JHEP **0111** (2001) 059 [hep-th/0111159].

[11] For a review, see: D. F. Litim and J. M. Pawlowski, hep-th/9901063.

[12] M. Reuter, Phys. Rev. D **57** (1998) 971 hep-th/9605030].

[13] A. Hasenfratz and P. Hasenfratz, Nucl. Phys. B **270** (1986) 687.

[14] A. Margaritis, G. Odor and A. Patkos, Z. Phys. C **39** (1988) 109.

[15] N. Tetradis and C. Wetterich, Nucl. Phys. B **422** (1994) 541 [hep-ph/9308214].

[16] T. R. Morris, Phys. Lett. **B329** (1994) 241 [hep-ph/9403340].

[17] R. D. Ball, P. E. Haagensen, J. I. Latorre and E. Moreno, Phys. Lett. **B347** (1995) 80.

[18] D. F. Litim and N. Tetradis, hep-th/9501042.

[19] N. Tetradis and D. F. Litim, Nucl. Phys. **B464** (1996) 492 [hep-th/9512073].

[20] J. Comellas and A. Travesset, Nucl. Phys. B **498** (1997) 539 [hep-th/9701028].

[21] T. R. Morris and M. D. Turner, Nucl. Phys. B **509** (1998) 637 [hep-th/9704202].

[22] S. B. Liao, J. Polonyi and M. Strickland, Nucl. Phys. **B567** (2000) 493 [hep-th/9905206].

[23] G. Von Gersdorff and C. Wetterich, Phys. Rev. B **64** (2001) 054513 [hep-th/0008114].

[24] D. F. Litim and J. M. Pawlowski, Phys. Lett. B **516** (2001) 197 [hep-th/0107020].

[25] O. Bohr, B.J. Schäfer and J. Wambach, Int. J. Mod. Phys. **A16** (2001) 3823 [hep-ph/0007098],
A. Bonanno and D. Zappalà, Phys. Lett. B **504** (2001) 181 [hep-th/0010095],
M. Mazza and D. Zappalà, Phys. Rev. D **64** (2001) 105013 [hep-th/0106230].

[26] S. B. Liao, Phys. Rev. **D53** (1996) 2020 [hep-th/9501124].

[27] D. F. Litim and J. M. Pawlowski, hep-th/0111191; hep-th/0202188.

[28] D. F. Litim, Phys. Lett. **B393** (1997) 103 [hep-th/9609040].

[29] F. Freire and D. F. Litim, Phys. Rev. D **64** (2001) 045014 [hep-ph/0002153].

[30] D. F. Litim, C. Wetterich and N. Tetradis, Mod. Phys. Lett. A **12** (1997) 2287,
B. Bergerhoff, D. F. Litim, S. Lola and C. Wetterich, Int. J. Mod. Phys. **A11** (1996) 4273,
B. Bergerhoff, F. Freire, D. F. Litim, S. Lola and C. Wetterich, Phys. Rev. **B53** (1996) 5734.

[31] O. Lauscher and M. Reuter, hep-th/0108040, hep-th/0110021;
M. Reuter and F. Saueressig, hep-th/0110054.

[32] T. R. Morris, Phys. Lett. B **334** (1994) 355 [hep-th/9405190].

[33] K. Aoki, K. Morikawa, W. Souma, J. Sumi and H. Terao, Prog. Theor. Phys. **99** (1998) 451.

[34] G. R. Golner, Phys. Rev. **B33** (1986) 7863.

[35] C. Wetterich, Z. Phys. C **57** (1993) 451.

[36] D. F. Litim and J. M. Pawlowski, Phys. Lett. B **435** (1998) 181 [hep-th/9802064]; hep-th/0203005.

[37] U. Ellwanger, M. Hirsch and A. Weber, Z. Phys. C **69** (1996) 687 [hep-th/9506019], B. Bergerhoff and C. Wetterich, Phys. Rev. D **57** (1998) 1591 [hep-ph/9708425].